

# Optical vehicular communication based on a-SiC:H technology

Manuel A. Vieira<sup>a,b</sup>, Manuela Vieira<sup>a,b,c,\*</sup>, Paula Louro<sup>a,b</sup>, Pedro Vieira<sup>a,d</sup>

<sup>a</sup> *Electronics Telecommunication and Computer Dept. ISEL/IPL, R. Conselheiro Emídio Navarro, 1949-014 Lisboa, Portugal*

<sup>b</sup> *CTS-UNINOVA, Quinta da Torre, Monte da Caparica, 2829-516 Caparica, Portugal*

<sup>c</sup> *DEE-FCT-UNL, Quinta da Torre, Monte da Caparica, 2829-516 Caparica, Portugal*

<sup>d</sup> *Instituto de Telecomunicações, Instituto Superior Técnico, 1049-001 Lisboa, Portugal*

Received 18 July 2017; accepted 28 May 2018

## Abstract

A smart vehicle lighting system that combines the functions of illumination, signaling, communications, and positioning is presented. A traffic scenario is established, and tested under ideal environment conditions. Vehicle-to-vehicle (V2V) and infrastructure-to-vehicle (I2V) communications are analyzed. For the V2V communication study, the emitter was developed based on the vehicle headlights, whereas for the study of I2V communication system, the emitter was built on the street-lights. The VLC receivers are located at the vehicle and are used to extract the data from the modulated light beam coming from the LEDs emitters. The VLC receiver is based on a-SiC:H technology and joins the simultaneous demultiplexing operation with the photodetection and self-amplification. The receiver and the transmitters are characterized through spectral response under different optical bias. The spectral sensitivity of the receiver and its optical gain are analyzed. An algorithm to decode the information is established. The experimental results confirmed that the proposed VLC architecture is suitable for the intended applications.

© 2018 Sociedade Portuguesa de Materiais (SPM). Published by Elsevier España, S.L.U. All rights reserved.

**Keywords:** a-SiC:H technology; LED; Visible light communication; Intelligent transportation system; Optical sensor; WDM

## 1. Introduction

Various modes of vehicular communications, such as infrastructure-to-vehicle (I2V), vehicle-to-vehicle (V2V) and vehicle-to-infrastructure (V2I) are becoming increasingly popular, boosted by navigation safety requirements and enabled by investments of car manufacturers [1].

Recently, LED-based optical wireless communication has been also proposed for infrastructure (street light, traffic lights) and car to car message delivery. This option turned to be particularly effective in short range direct communications to explore Line-of-sight (LoS) and overcome the issues related to the isotropic nature of radio waves. One additional benefit of LEDs is that they can switch to different light intensities at a very fast rate. This functionality has given rise to a novel communication technology (Visible Light Communication – VLC) where LED

luminaires can be used for lighting purposes and high speed data transfer [2,3].

In the recent past, we have developed a Wavelength Division Multiplexer (WDM) device that improves the transmission capacity of the optical communications, in the visible range. The device was based on tandem a-SiC:H/a-Si:H pin/pin light controlled filter. When different visible signals are encoded in the same optical transmission path [4,5] the device multiplexes the different optical channels, performs different filtering processes (amplification, switching, and wavelength conversion) and decodes the encoded signals recovering the transmitted information. This device can be used as receiver and can help to develop automated vehicle technologies that allow cars to communicate with the ‘environment’ around them [6].

In this paper, a traffic scenario is established. The transmitters and the receivers are characterized and the main optoelectronic properties analyzed. The performances of the cooperative driving system integrating the transmitter and the receiver are evaluated. To achieve vehicular communication (V2V or I2V) 4 bit string color messages in the visible range and their three

\* Corresponding author.

E-mail address: [mv@isel.ipl.pt](mailto:mv@isel.ipl.pt) (M. Vieira).

parity bits for error control and ID address are used to transmit a codeword that is received and decoded by the a-SiC:H pin'/pin receiver. Code and parity MUX/DEMUX signals are transmitted and analyzed. As proof of concept a traffic scenario is established and tested.

## 2. Experimental

A VLC system mainly consists of a VLC transmitter that modulates the light produced by LEDs and a VLC receiver based on a photosensitive element that is used to extract the modulated signal from the light. The transmitter and the receiver are physically separated, but connected through the VLC channel. For VLC systems, the LoS is a mandatory condition.

### 2.1. VLC transmitter

The use of trichromatic RGB-LEDs as transmitters offers the possibility of WDM which greatly increases the transmission data rate. They are used for lighting purposes and, when modulated, to transmit data. We use commercially available violet (V: 400 nm) and white RGB-LEDs. The output spectra of the white LED contains three peaks assigned to the colors red (R: 626 nm), green (G: 530 nm) and blue (B: 470 nm) that mixed together provide the white perception to the eye. They exhibit a wide divergence angle ( $2 \times 60^\circ$ ), since they are also designed for general lighting and allows a wide delivery of the VLC signal around the surrounding area. The white LEDs require three separate driver circuits to realize the white light. To decrease this complexity, only one chip of the LED is modulated for data transmission, the red, the green or the blue while the other two are provided constant current for illumination. In Fig. 1a the normalized emission spectra of each single chip is displayed. Each R, B or G chip can be switched *on* and *off* individually for a desired bit sequence. Here 1 means that the light is on 0 that is off. An extra violet modulated LED [V] was added to increase data transmission and to generate parity bits [7] that allow error control. A seven bit code is used to transmit the information. The encoder takes four input data bits [R G B V] and generates three additional parity bits, *i.e.*, the parity bits are SUM bits of the three-bit additions of violet pulsed signal with two additional bits of RGB [8] and are given by:

$$P_R = V + R + B \quad (1)$$

$$P_G = V + R + G \quad (2)$$

$$P_B = V + G + B \quad (3)$$

Moreover, the seven-bit codeword will be in a format, with the data and the parity bits [R G B V;  $P_R$   $P_G$   $P_B$ ] separated. To transmit the data an On-Off Keying (OOK) code was used.

Taking into account Eqs. (1)–(3), in Fig. 1b, an example of the digital signals (codewords) used to drive the LEDs are displayed. All the sixteen ( $2^4$ ) *on/off* possible combinations of the four R, G, B and V input channels are reported as solid lines and the correspondent parity bits as dotted lines. The arrow exemplifies the seven [1111:111] and [1001:001] bit codewords.

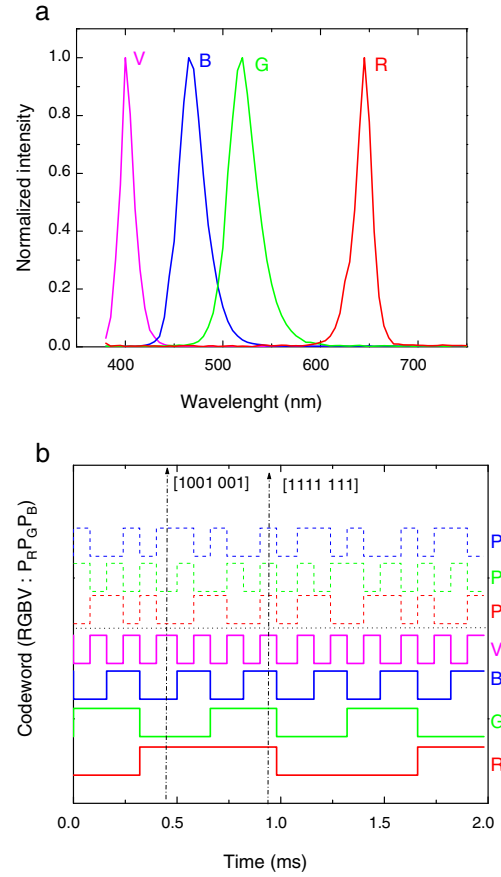


Fig. 1. (a) Normalized spectra of the RGBV input channels. (b) Representation of the original encoded message [R G B V;  $P_R$   $P_G$   $P_B$ ].

### 2.2. VLC receiver

The VLC receiver is used to extract the data from the modulated light beam. It transforms the light into an electrical signal that will be demodulated and decoded by the receiver.

The VLC receiver is a tandem, p-i'(a-SiC:H)-n/p-i(a-Si:H)-n heterostructure produced by PECVD (Plasma Enhanced Chemical Vapour Deposition) sandwiched between two transparent conductive contacts (TCO). The device configuration is shown in Fig. 2. The intrinsic layer of the front p-i'-n photodiode is made of a-SiC:H while the back intrinsic layer is based on a-Si:H. The deposition conditions and optoelectronic characterization of the single layers and device, as well as their optimization, were described in previous papers [4,9]. The thickness (200 nm) and the optical gap (2.1 eV) of the a-SiC:H intrinsic layer (i'-) is optimized for blue collection and red transmittance. The thickness (1000 nm) of the a-Si:H i-layer was adjusted to achieve full absorption in the green and high collection in the red ranges. As a result, both front and back diodes act as optical filters confining, respectively, the optical carrier produced by the blue and red photons respectively in the front and back photodiodes, while the optical carriers generated by the green photons are absorbed across both.

The device operates within the visible range using for data transmission the square wave modulated low power light sup-

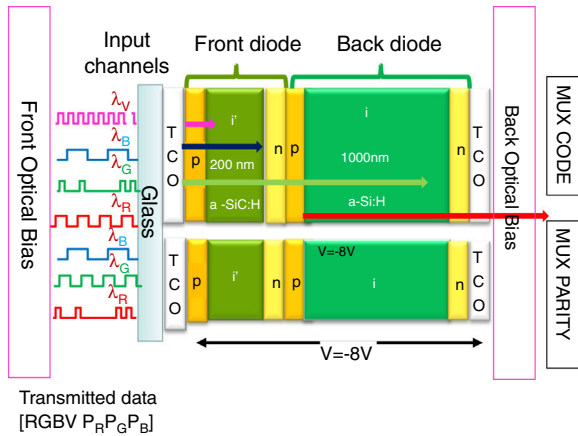


Fig. 2. Receiver configuration and operation.

plied by a violet and a trichromatic red (R), green (G), blue (B) and violet (V) LED. In this experiment, a mixture of red, green, blue and violet;  $\lambda_{R,G,B,V}$ ; pulsed communication channels (input channels; transmitted data), each one with a specific bit sequence (payload data), impinge on the device and are absorbed accordingly to their wavelengths (see arrow magnitudes in Fig. 2). The combined optical signal (multiplexed signal; received data) is analyzed by reading out the generated photocurrent under negative applied voltage ( $-8$  V), with and without 390 nm front and back background lighting, [10].

In Fig. 3a, the measured signal due to the overlap of the four independent input channels (MUX signal) is displayed without applied optical bias (dark) and under front and back irradiation. On the top, the driving signal applied to each R, G, B and V LED is presented, the bit sequence was chosen in order that when one channel is *on* the others are always *off*. In Fig. 3b, the spectral gain, defined as the ratio between the photocurrent with and without applied optical bias, is displayed under front and back irradiation. In Fig. 3c, the MUX signal due to the reception of four R, G, B, and V input channels is shown under front and back lighting. The drive signals applied to each transmitter are displayed in the top. The bit sequence was chosen in order that all the possible sixteen *on/off* combinations are allowed.

Data shows that the photocurrent depends on the irradiated side and on the incoming wavelength, acting the irradiation side as optical selector for the input channels. Under front irradiation, the long wavelength channels are enhanced and the short wavelength channels quenched while the opposite occurs under back irradiation. The device acts as an active long-pass filter under front irradiation and a low-pass filter under back irradiation. Under front bias the gain is higher than the unity for wavelengths above 500 nm resulting in an amplification of the green and red spectral ranges. Back irradiation only amplifies the short wavelength range and extinguishes the others. This nonlinearity is the main idea for the decoding of the MUX signal. Front violet bias is absorbed at the top of the front diode, increasing the electric field at the back diode, due to the self bias effect [11] where the red and part of the green incoming photons are absorbed (see Fig. 2). Under back irradiation the electric field

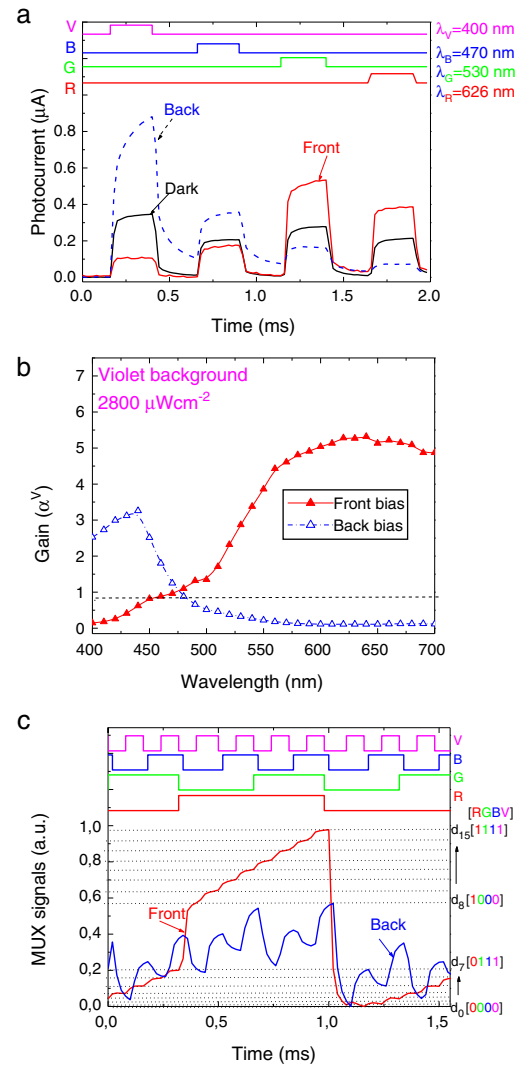


Fig. 3. (a) Transient photocurrent without (dark) and under front (front) and back (back) 390 nm irradiation. (b) Spectral gain under violet optical bias ( $\alpha^V$ ). (c) MUX signal under front and back 390 nm irradiation.

increases mainly near the front p-n interface, where the violet and part of the blue incoming channels generate most of the photocarriers. So, by switching between front to back irradiation, the photonic function is modified from a long- to a short-pass filter allowing, alternately selecting the long or the short wavelength channels.

Results (Fig. 3c) show that, under front irradiation, to each *on/off* possible combination corresponds a separate level. Here, all the sixteen levels ( $d_0$ – $d_{15}$ ) are detected and grouped into two main classes due to the high amplification of the red channel ( $\alpha^V_R \gg 1$ ). The upper eight ( $d_8$ – $d_{15}$ ) are ascribed to the presence of the red channel ( $R = 1$ ), and the lower eight ( $d_0$ – $d_7$ ) to its absence ( $R = 0$ ), having the device a long-pass filter function. In the right side of Fig. 3c the 4-binary code ascribed to the different levels (horizontal dotted lines) is pointed out. Under back irradiation, the same encoded multiplexed signal is, also, made of sixteen sublevels but grouped into different main levels, in the eight maximums the violet channel is *on* ( $V = 1$ ) and at the eight minimums it is *off* ( $V = 0$ ), having the device a short-pass filter

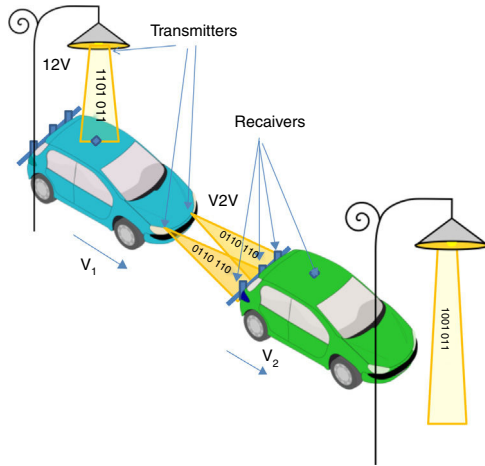


Fig. 4. Illustration of the proposed scenario: V2V and I2V hybrid systems.

function. Due to the quenching of the violet signal under front irradiation two consecutive levels, can present similar magnitudes. To avoid errors in the decoding process, in Section 3.1, the error control was done using only front irradiation and the parity check bits control [8].

### 2.3. VLC architecture

A infrastructure to vehicle (I2V) follow by vehicle to vehicle (V2V) communication was simulated and its architecture displayed in Fig. 4. In the simulation, the environmental noises and real traffic conditions were not taken into account.

In the I2V communication, the emitter was developed based on street lights, located on roadside, and the transmitted information received and decoded in the SiC pi npin device, located in the car roof. The street lights emit light signals within a capture range across one or more road lanes. When a probe vehicle enters the street light's capture range, the receivers in the probe vehicles respond to light signal and its unique ID and traffic message are assigned. They send a codeword message [RGBV:  $P_R$ ,  $P_G$ ,  $P_B$ ] composed by red, green, blue and violet 4-binary bits (four input data bits [R G B V]) and generate three additional parity bits [ $P_R$ ,  $P_G$ ,  $P_B$ ] for easy decoding and error control [12]. This data is then transmitted to the others vehicles (V2V communication). Hence, the transmitter can send a traffic message that is receive by the follower and retransmitted to the others vehicles.

To build the V2V system that allows feedback channel between leader vehicle and follower vehicle, the follower vehicle is equipped with two headlamps transmitters. The leader vehicle is assumed to be equipped with three a-SiC pinpin receivers to detect optical messages, as in Fig. 4. The spacing of the two transmitters is fixed while their distance to the receivers varies and dependent on the speed ( $v_1$ ,  $v_2$ ). Both transmitters are oriented towards the receivers. Here, the follower vehicle sends the message that is received by the leader and can be retransmitted for the next car. Experiments were conducted on straight and not on turning and zigzag paths.

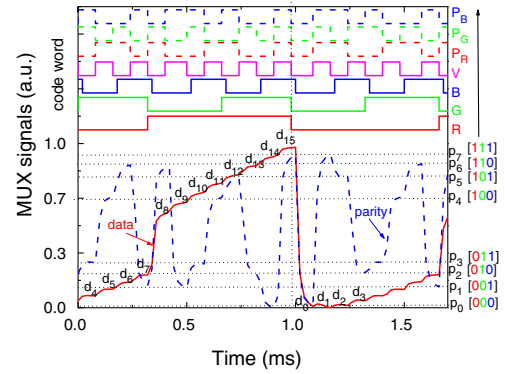


Fig. 5. Code and parity MUX/DEMUX signals under 390 nm front irradiation. On the top the transmitted channels [R G B V:  $P_R$   $P_G$   $P_B$ ] are decoded.

## 3. Results and discussion

### 3.1. Multiplexing/demultiplexing techniques

For an optoelectronic digital capture system, opto-electronic conversion is the relationship between the optical inputs and the corresponding digital output levels. Whereas the multiplexer is a data selector, the demultiplexer is a data distributor or data router. Just as the multiplexer has a binary code (RGBV) for the selection of an input, the demultiplexer has a similar code for selecting a particular output.

In Fig. 5, the received data, *i.e.*, the MUX code signal in the same stamp time of Fig. 3c, due to the combination of the four R, G, B, and V input channels and the correspondent parity bits are displayed, under front irradiation. The solid line shows the MUX code signal and the dash lines the synchronized parity MUX signal transmitted with the data code.

The MUX signal presents as much separated levels as the *on/off* possible combinations of the input channels, allowing decoding the transmitted information. All the possible sixteen ordered levels ( $d_0$ – $d_{15}$ ) are pointed out at the correspondent levels, and the ordered eight parity levels ( $p_0$ – $p_7$ ) ascribed to the parity bits are displayed as horizontal dotted lines. In the right hand of Fig. 5, the correspondence between the parity levels and the parity bits is shown (see Fig. 1). In the top, the decoded seven bit word [R, G, B, V:  $P_R$ ,  $P_G$ ,  $P_B$ ] of the transmitted inputs is displayed. Results show that to each of the  $2^n$  possible *on/off* states corresponds to a well-defined level. Hence,  $2^4$  ordered levels are detected ( $d_0$ – $d_{15}$ ) and correspond to all the possible combinations of the *on/off* states [13]. Taking into account Fig. 3, under front irradiation, each of those  $n$  channels is enhanced or quenched differently, resulting in an increase of red/green magnitude and a decrease on the blue/violet magnitude. Hence, by assigning each output level to a  $n$  digit binary code (weighted by the optical gain of the each channel), [ $X_R$ ,  $X_G$ ,  $X_B$ ,  $X_V$ ], with  $X = 1$  if the channel is *on* and  $X = 0$  if it is *off*, the signal can be decoded.

The proximity of the magnitude of consecutive levels causes occasional errors in the decoded information that are corrected using the parity bits. For instance, levels  $d_1$ ,  $d_2$ , and  $d_3$  have similar magnitude and can be confused when reading a word

message, however their parity levels, respectively,  $p_7$ ,  $p_5$  and  $p_2$ , are different. The parity of the word is checked after reading the word. The word is accepted if the parity of the bits read out is correct. If the parity of the bits is incorrect, an error is detected and should be corrected. Experimental results show that the use of trichromatic RGB LED as transmitters and a-SiC:H pi-npin optical processors as receivers allow the use of multiplex/demultiplex techniques that increase the transmission rate. A maximum transmission rate capability of 30 kbps was achieved.

### 3.2. Vehicular system evaluation

A traffic scenario was established for the I2V and V2V communication. The proof of concept is simulated and depicted in Fig. 6a. Here, the geometrical relation between the two vehicles (leader vehicle and follower vehicle) and the distances between them (A, B and C) are displayed. It shows the inter-vehicle distance decreasing as total photocurrent on the three receivers changes. The street light sends a coded message (traffic message) that includes its ID (violet channel) and traffic information (RGB channels). This message is received and decoded by the follower vehicle and retransmitted to the leader.

In Fig. 6b, the I2V MUX data (solid line) and parity (dash line) signals received by the roof sensor are displayed. In top the decoded signal is shown. After decoding the follower vehicle sends the information using the modulated light from the headlamps forming a lighting coverage. The leader vehicle receives and decodes the message in three separated receivers at the tail and compares them. It was assumed that each LED chip sends light only perpendicular to the semiconductor's surface, and a few degrees to the side, which results in a light cone pattern.

Here, three situations are possible: A, the vehicles are in a safety distance and the three sensors receive the same message with the same intensity; B, the vehicles are in a warning distance, they are approaching and the left and the right sensor receive the same message but at the middle sensor the message arrives with double intensity; C, the vehicles are too close, in the automatic braking distance, and the same message arrives to the left and to the right sensor and no message is read out by the middle one. Based on that, the driving range distance can be calculated and a warning can be sent to the driver or activates the automatic braking system. We have simulated the scenario B (see Fig. 6a), the drive current applied to the two RGB-LEDs (headlamps-like) was the same and adjusted in order to have the same lighting conditions of this region.

In Fig. 6c, the V2V MUX signals received on the right (R) and left (L) sensors or in the middle (M) one are displayed. The solid lines are ascribed to the MUX data word and the dash lines, to the correspondent parity MUX. The same 4:3 binary information (on the top of the figure) was sent simultaneously by both LEDs.

Results show that, the right and the left sensor receive the same message and the one in the middle receives the overlap of both. We have applied to the RGB LED a current of the order of 4 mA and 30 mA to the violet one. As expected, the shape of both code and parity MUX signals are the same but the intensity

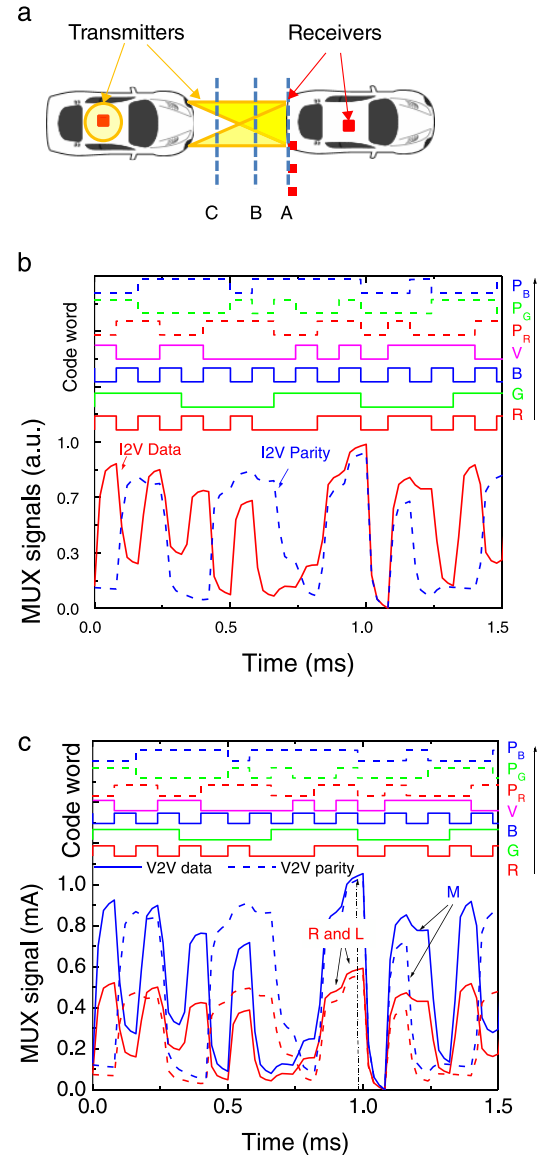


Fig. 6. Proof of concept: (a) Driving range scenario. (b) Signals acquired in a I2V communication, MUX (solid line) and parity (dash line) signals. (c) Signals acquired by the R (right); L (left); and M (middle) receivers in a V2V communication, MUX (solid line) and parity (dash line) signals.

in the middle sensor ( $\cong 1 \mu\text{A}$ ) is almost twice of the one received in the two others ( $\cong 0.5 \mu\text{A}$ ).

### 4. Conclusion and future trends

An optical vehicular communication system that integrates I2V and V2V VLC prototypes is presented. The system incorporates VLC transmitters that modulate the light produced by white RGB-LEDs, and by VLC receivers, based on photo-sensitive elements (a-SiC:H pi-npin photodiodes), that code and decode the emitted modulated signals. The optoelectronic characterization from the emitters and receivers is presented. Multiplexing/demultiplexing techniques are tested and an algorithm to decode the transmitted information is developed. As proof of concept a traffic scenario is established and tested under

ideal conditions. No environmental noises or real traffic conditions were taken into account. Results show that the cooperation between the two allows the road-side-unit to communicate with vehicles outside its service area. The results are highly improved by integration error correcting codes. In order to move towards real implementation, the performance of such systems still needs improvement. As a future goal, we plan to finalize the embedded application, for experimenting in several road configurations with either static or moving vehicles.

## Acknowledgements

This work was sponsored by FCT – Fundação para a Ciência e a Tecnologia, within the Research Unit CTS – Center of Technology and systems, reference UID/EEA/00066/2013 and by the projects IPL/2016 /VLC\_MIMO/ISEL and 2017/SMART\_VeDa/ISEL. IPL/2017.

## References

- [1] S. Yousefi, E. Altman, R. El-Azouzi, M. Fathy, Analytical model for connectivity in vehicular ad hoc networks, *IEEE Trans. Vehic. Technol.* 57 (2008) 3341–3356.
- [2] S. Schmid, G. Corbellini, S. Mangold, T.R. Gross, An LED-to-LED visible light communication system with software-based synchronization, in: 2012 IEEE Globecom Workshops, 2012, pp. 1264–1268.
- [3] D. O'Brien, H.L. Minh, L. Zeng, G. Faulkner, K. Lee, D. Jung, Y. Oh, E.T. Won, Indoor visible light communications: challenges and prospects, *Proc. SPIE* 7091 (2008) 709106.
- [4] M. Vieira, P. Louro, M. Fernandes, M.A. Vieira, A. Fantoni, J. Costa, Three transducers embedded into one single SiC photodetector: lsp direct image sensor, optical amplifier and demux device, in: *Advances in Photodiodes*, InTech, 2011, pp. 403–425 (Chapter. 19).
- [5] M.A. Vieira, P. Louro, M. Vieira, A. Fantoni, A., A. Steiger-Garção, Light-activated amplification in Si-C tandem devices: a capacitive active filter model, *IEEE Sens. J.* 12 (6) (2012) 1755–1762.
- [6] M.A. Vieira, M. Vieira, P. Vieira, P. Louro, Optical signal processing for a smart vehicle lighting system using a-SiCH technology, in: *Proc. SPIE* 10231, *Optical Sensors 2017*, 2017, May, pp. 102311L.
- [7] R.W. Hamming, Error detecting and error correcting codes, *Bell Syst. Tech. J.* 29 (1960) 147–160.
- [8] M.A. Vieira, M. Vieira, V. Silva, P. Louro, J. Costa, Optical signal processing for data error detection and correction using a-SiCH technology, *Phys. Status Solidi C* 12 (12) (2015) 1393–1400.
- [9] M.A. Vieira, P. Louro, M. Vieira, A. Fantoni, A. Steiger-Garção, Light-activated amplification in Si-C tandem devices: a capacitive active filter model, *IEEE Sens. J.*, 12 (6) (2012) 1755–1762.
- [10] M. Vieira, A. Fantoni, P. Louro, M. Fernandes, R. Schwarz, G. Lavareda, C.N. Carvalho, Self-biasing effect in colour sensitive photodiodes based on double p-i-n a-SiC:H heterojunctions, *Vacuum* 82 (12) (2008) 1512–1516.
- [11] M.A. Vieira, M. Vieira, P. Louro, V. Silva, Error detection on a spectral data using an optical processor based on a-SiC technology, *Sens. Transducers* 184 (January (1)) (2015) 116–122, © 2015 by IFSA Publishing, S. L. (2015).
- [12] M.A. Vieira, M. Vieira, V. Silva, P. Louro, M. Barata, Optoelectronic logic functions using optical bias controlled SiC multilayer devices, *MRS Proc.* 1536 (2013) 91–96.